

Supporting Information

Facile preparation of single-atom Ru catalysts via two-dimensional interface directed synthesis technique for NRR

Yao Chen^{‡a}, Rui Xu^{‡*a}, Yuchao Li^{*a}, Lu Cai^a, Yubo Yang^a, Yanxia Zheng^a, Cuncun Zuo^a, Haofei Huang^a, Zijian Wen^a, and Qian Wang^b

a. Cleaning Chemical Research Institute, School of Chemistry and Chemical Engineering, Shandong University of Technology, Zibo, Shandong 255000, China

b. College of Chemistry, Chemical Engineering and Materials Science, Shandong Normal University, Jinan Shandong 250014, China.

E-mail: ruixu@sdut.edu.cn, cyulee@126.com

‡These authors contributed equally to this work and should be considered co-first authors.

1. Experimental procedures

1.1 Materials

Nafion 117 (5 wt%) solution, ruthenium (III)-2,4-pentanedionate ($C_{15}H_{21}O_6Ru$), tetraacetoxysilane ($C_8H_{12}O_8Si$), 3-aminopropyltrimethoxysilane ($C_6H_{17}NO_3Si$, ATPMS) and dicyandiamide ($C_2H_4N_4$) were purchased from Aladdin Ltd. (Shanghai, China). Hydrochloric acid (HCl), potassium permanganate ($KMnO_4$), sulfuric acid (H_2SO_4), sodium nitrate ($NaNO_3$), ammonium hydroxide ($NH_3 \cdot H_2O$) and sodium hydroxide (NaOH) were purchased from Sinopharm Chemical Reagent Co., Ltd. Graphite powder were purchased from Qingdao Huatai Lubricating and Sealing Technology Co., Ltd. Ethyl Alcohol were purchased from Shanghai Titan Technology Co., Ltd. Acetone were purchased from Shanghai Dahe Chemicals Co., Ltd. Carbon paper were bought from Guangdong Canrd New Energy Technology Co., Ltd. The ultrapure water used throughout all experiments was purified through a UP system. All reagents were analytical reagent grade without further purification.

1.2 Preparation of rGO/NC

1 g fully ground SiO_2 spheres (prepared by Stober method¹) were mixed in 500 mL ethanol and 5 mL ATPMS, washed after 5 h reaction at 45°C and then 25 mL deionized water was added (SiO_2 -amination). 250 ml GO (prepared by Hummers method²) aqueous solution ($0.2 \text{ mg} \cdot \text{ml}^{-1}$) was prepared and crushed for 2 h. The above two solutions were mixed and stirred for 1 h, and then centrifuged, washed and dried to obtain SiO_2/GO . 15 g dicyandiamide was dissolved in 60 mL deionized water at 80°C, and 1 g SiO_2/GO was added into the solution and stirred for 12 h. The mixture was transferred to the reactor and heated at 140°C for 5 h. After filtering, washing and drying, the mixture was calcined under N_2 atmosphere at 900°C for 1h to obtain $SiO_2/rGO/NC$. The ground $SiO_2/rGO/NC$ powder was placed at 50°C in 4 M NaOH for 24 h, filtered, washed, and dried to produce hollow rGO/NC nanospheres.

1.3 Preparation of SA-Ru@rGO/NC

200 mg hollow rGO/NC nanospheres were added to a round-bottomed flask filled with N_2 . Ruthenium (III)-2,4-pentanedionate was dissolved in acetone solution (4

mg·ml⁻¹), titrated into a round bottom flask and dried for 24h to obtain Ru@rGO/NC₁ (0.75 wt%), Ru@rGO/NC (ie, SA-Ru@rGO/NC, 0.95 wt%), and Ru@rGO/NC₂ (1 wt%).

1.4 Electrochemical measurements

Electrochemical measurements were performed with a CH760E electrochemical analyzer (CH Instruments, Inc., Shanghai) using a standard three-electrode system using Ag/AgCl electrode as the reference electrode, platinum net as the counter electrode, Ru@rGO/NC as the working electrode, and HCl as the electrolyte. The test potential can be converted into a reversible hydrogen electrode potential according to the potential correction equation: $E_{\text{RHE}} = E_{\text{Ag/AgCl}} + 0.059 \text{ PH} + 0.222 \text{ V}$. All potentials in this experiment were represented in the form of a reversible hydrogen electrode potential.

Before NRR tests, the Nafion 117 membrane was pre-treated by heating in 5% H₂O₂ solution and 5% H₂SO₄ solution at 80 °C for 1 h, respectively. In a typical electrode synthesis, weighed 5 mg catalyst and add 0.7 ml of water and 0.3 ml of ethanol and stirred well. Added 30 μl of 5% Nafion and stirred well (System 1: 1.4 ml of water, 0.6 ml of ethanol, then added 60 μl of 5% Nafion, stirred evenly), and then applied the prepared slurry to the carbon paper and dried it well.

In addition, high-purity nitrogen was purged for at least 30 min before starting the test, followed by NRR testing at different potentials (-0.1 V, -0.15 V, -0.2 V, -0.25 V, -0.3 V, -0.35 V, -0.4 V, -0.45 V, -0.5 V). The LSV curve was a steady-state curve obtained after multiple cyclic scans at 1 mV s⁻¹.

1.5 Characterizations

TEM images were obtained from the JEM-1400plus High Resolution Transmission Electron Microscopy and the JEM-ARM300F Spherical Aberration Corrected Transmission Electron Microscope. XPS measurements were performed with the K-Alpha X-ray photoelectron spectrometer using Mg as the exciting source. All spectra were calibrated to the C 1s binding energy at 284.8 eV. The UV-vis absorbance data of the resulted samples were tested by using the UV-vis spectrophotometer (UV-2600). N₂ gas sorption isotherms were determined using the

gas sorption instrument (ASAP2460, USA). The specific surface area data were determined by the Brunauer-Emmett-Teller method. Pore size distributions of samples were obtained according to BJH theory.

1.6 Determination of NH₃

Concentration of produced ammonia was spectrophotometrically determined by the indophenol blue method. Absorbance measurements were performed at $\lambda = 660$ nm. The concentration-absorbance curves were calibrated using standard solution with a series of concentrations (1.5 $\mu\text{g}\cdot\text{mL}^{-1}$, 1.2 $\mu\text{g}\cdot\text{mL}^{-1}$, 0.9 $\mu\text{g}\cdot\text{mL}^{-1}$, 0.6 $\mu\text{g}\cdot\text{mL}^{-1}$, 0.3 $\mu\text{g}\cdot\text{mL}^{-1}$), which contained the same concentrations of HCl as used in the electrolysis experiments. The measurements with the background solutions (no NH₃) were conducted for all experiments, and the background peak absorbance was subtracted from the measured peak absorbance of NRR experiments to estimate the NH₃ concentrations and the faradaic efficiencies. The fitting curve ($y = 0.36333x - 0.01525$, $R^2 = 0.99935$) shows good linear relation of absorbance value with NH₃ concentration.

1.7 Determination of N₂H₄

The formation of hydrazine during electrolysis was examined by the method of Watt-Chrisp. The mixture solution of 5.99 g C₉H₁₁NO, 30 mL HCl and 300 mL ethanol was used as a color reagent. Typically, 5 mL electrolyte was removed from the electrochemical reaction vessel, and added into 5 mL above prepared color reagent 10 min at room temperature. Moreover, the absorbance of the resulting solution was measured at a wavelength of 455 nm. The concentration-absorbance curves were calibrated using standard N₂H₄ solution with a series of concentrations (5.0 $\mu\text{g}\cdot\text{mL}^{-1}$, 4.0 $\mu\text{g}\cdot\text{mL}^{-1}$, 2.0 $\mu\text{g}\cdot\text{mL}^{-1}$, 1.0 $\mu\text{g}\cdot\text{mL}^{-1}$, 0.4 $\mu\text{g}\cdot\text{mL}^{-1}$). The fitting curve ($y = 0.69662x - 0.00102$, $R^2 = 0.99997$) shows good linear relation of absorbance value with N₂H₄ concentration.

1.8 Calculations of NH₃ formation rate and FE

The yield rate of NH₃ can be estimated using the following equation:

$$r(\text{NH}_3) = n(\text{NH}_3) / (t \times m_{\text{cat}})$$

where n_{NH_3} is the ammonia yield, t is the electrolysis time, and m is the metal mass or the total mass of the catalyst.

The FE was calculated from the charge consumed for NH₃ generation and the total charge passed through the electrode::

$$\text{FE (NH}_3\text{) \%} = 3 \times n(\text{NH}_3) \times F / Q$$

where F is the faraday constant (96485.3 C mol⁻¹), Q is the total charge passed through the electrode, “3” represents the number of electrons transferred per NH₃.

1.9 Density functional theory (DFT) Calculation

The present first principle DFT calculations are performed by Vienna Ab initio Simulation Package (VASP)³ with the projector augmented wave (PAW) method⁴. The exchange-functional is treated using the generalized gradient approximation (GGA) of Perdew-Burke-Emzerhof (PBE)⁵ functional. The energy cutoff for the plane wave basis expansion was set to 450 eV and the force on each atom less than 0.03 eV/Å was set for convergence criterion of geometry relaxation. Grimme’s DFT-D3 methodology⁶ was used to describe the dispersion interactions. Partial occupancies of the Kohn–Sham orbitals were allowed using the Gaussian smearing method and a width of 0.05 eV. The Brillouin zone was sampled with Monkhorst mesh 3 × 3 × 1 through all the computational process. The self-consistent calculations apply a convergence energy threshold of 10⁻⁵ eV. A 15 Å vacuum space along the z direction was added to avoid the interaction between the two neighboring images.

The adsorption energy (E_{ads}) of adsorbate N₂ was defined as

$$E(\text{ads}) = E(\text{N}_2/\text{surf}) - E(\text{surf}) - E(\text{N}_2(\text{g}))$$

where E(N₂/surf), E(surf) and E(N₂(g)) are the energy of adsorbate N₂ adsorbed on the surface, the energy of clean surface, and the energy of isolated N₂ molecule in a cubic periodic box, respectively.

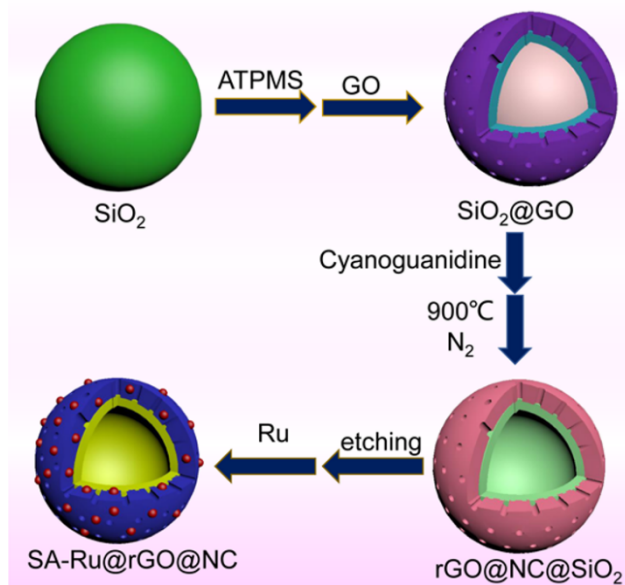


Fig. S1 The synthesis process of SA-Ru@rGO/NC.

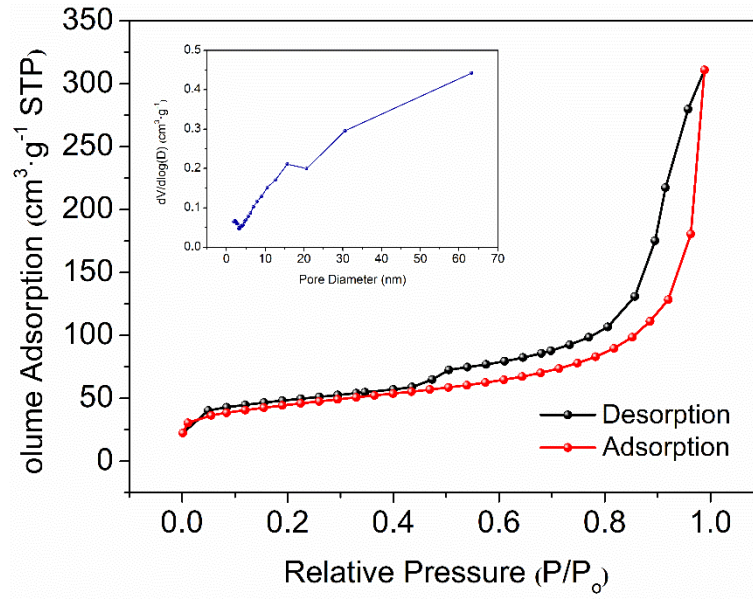


Fig. S2 N₂ adsorption–desorption isotherms and the corresponding pore size distribution curves for rGO/NC.

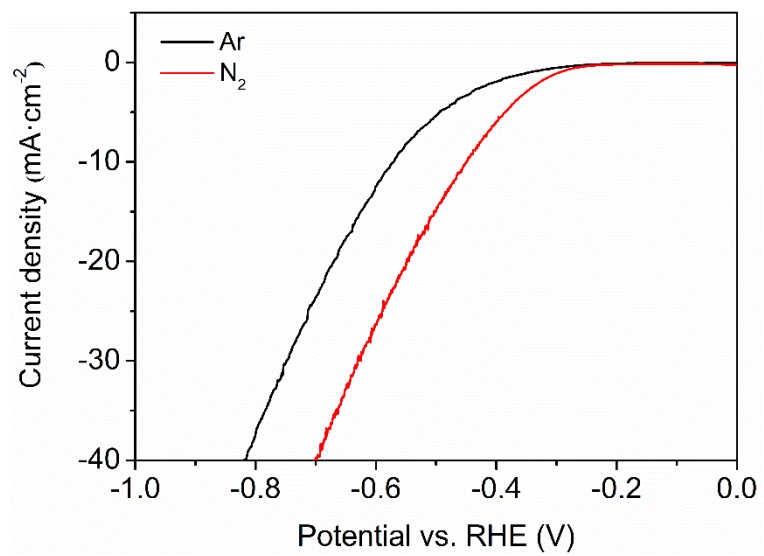


Fig. S3 LSV curves of SA-Ru@rGO/NC at 1 mV·s⁻¹.

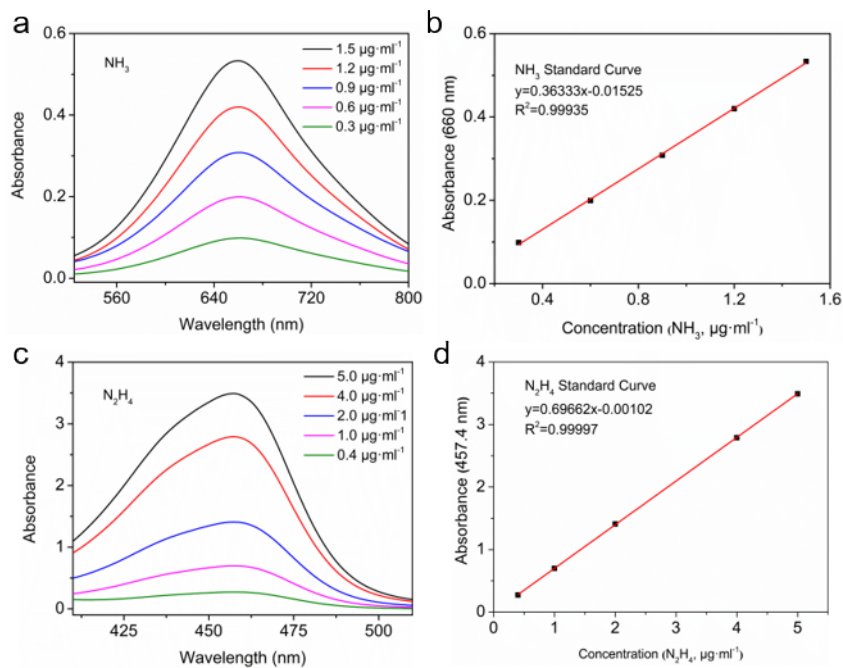


Fig. S4 (a) UV-Vis curves of various NH_3 concentrations. (b) Calibration curve used for estimation of NH_3 . (c) UV-Vis curves of various N_2H_4 concentrations. (d) Calibration curve used for estimation of N_2H_4 .

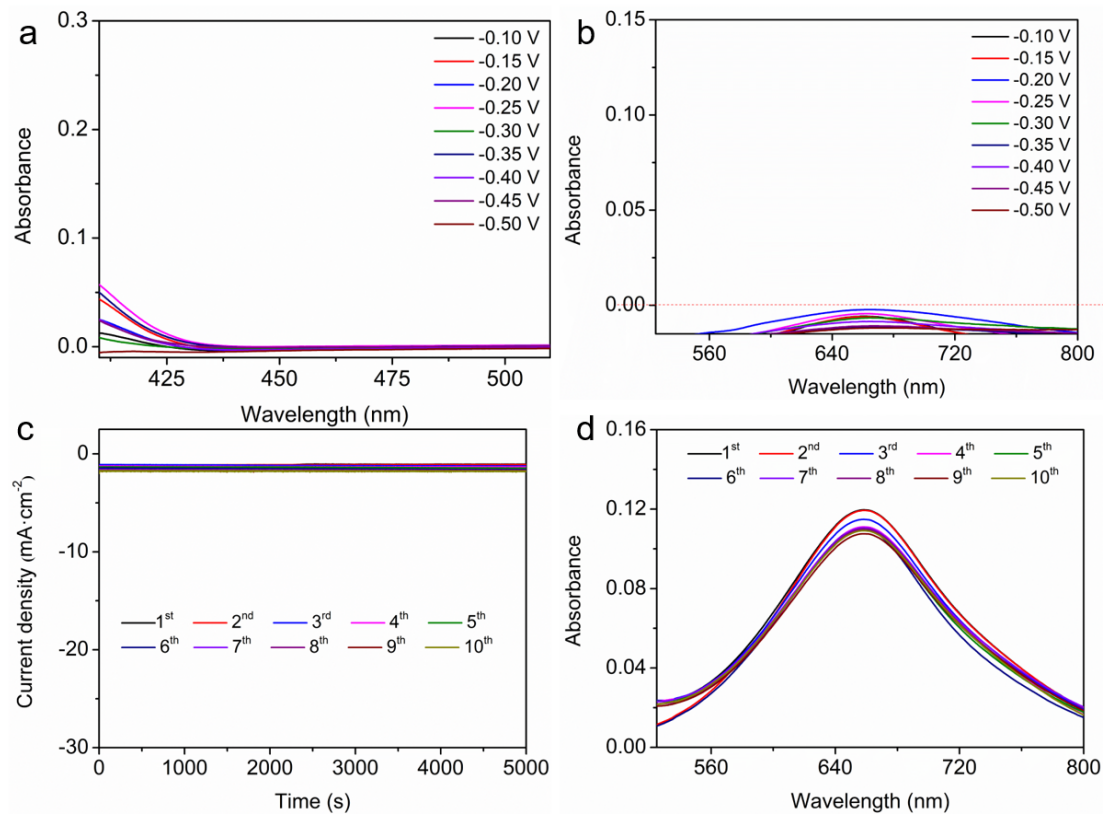


Fig. S5 (a) The UV-Vis curves of the N_2H_4 corresponding to the SA-Ru@rGO/NC at different potentials in N_2 -saturated. (b) The UV-Vis curves of the NH_3 corresponding to the SA-Ru@rGO/NC at different potentials in Ar-saturated. (c) Time-dependent current density curves of SA-Ru@rGO/NC at -0.3 V for continuous cycles. (d) UV-Vis curves of the electrolytes stained with NH_3 color agent at -0.3 V for continuous cycles.

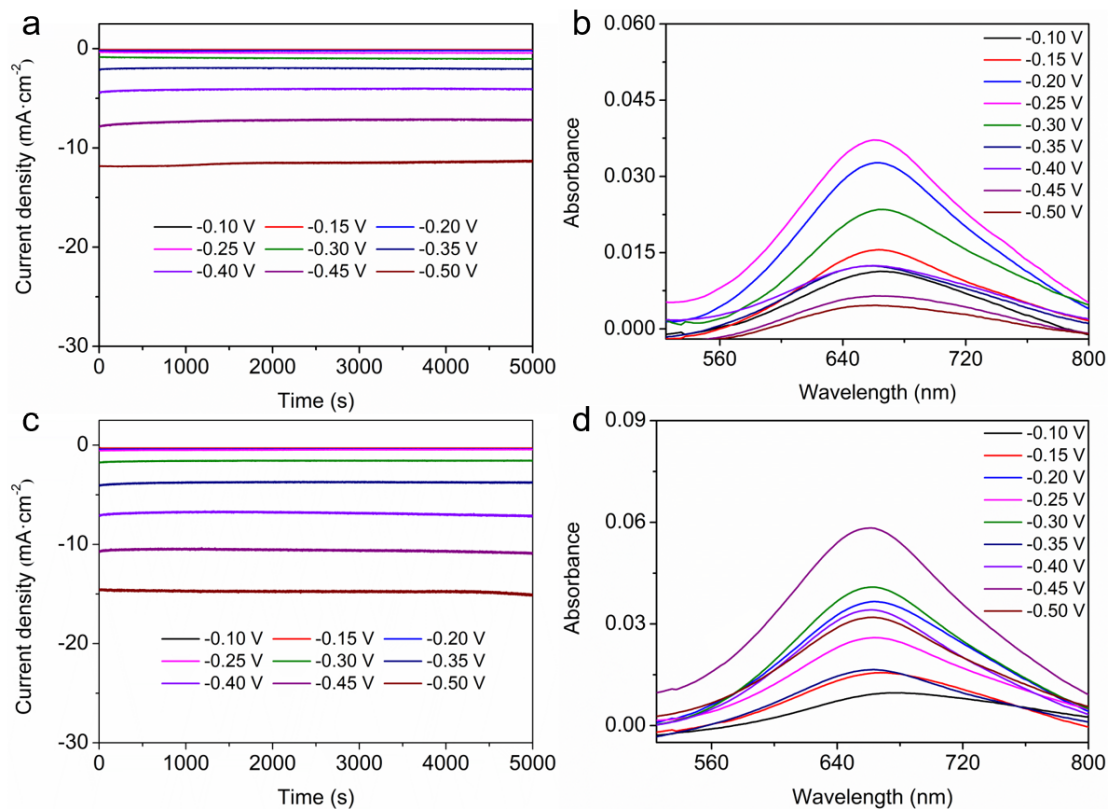


Fig. S6 (a) The It curves in N₂-saturated at different potentials for Ru@rGO/NC₁. (b) The corresponding UV-Vis curves of NH₃ in N₂-saturated at different potentials for Ru@rGO/NC₁. (c) The It curves in N₂-saturated at different potentials for Ru@rGO/NC₂. (d) The corresponding UV-Vis curves of NH₃ in N₂-saturated at different potentials for Ru@rGO/NC₂.

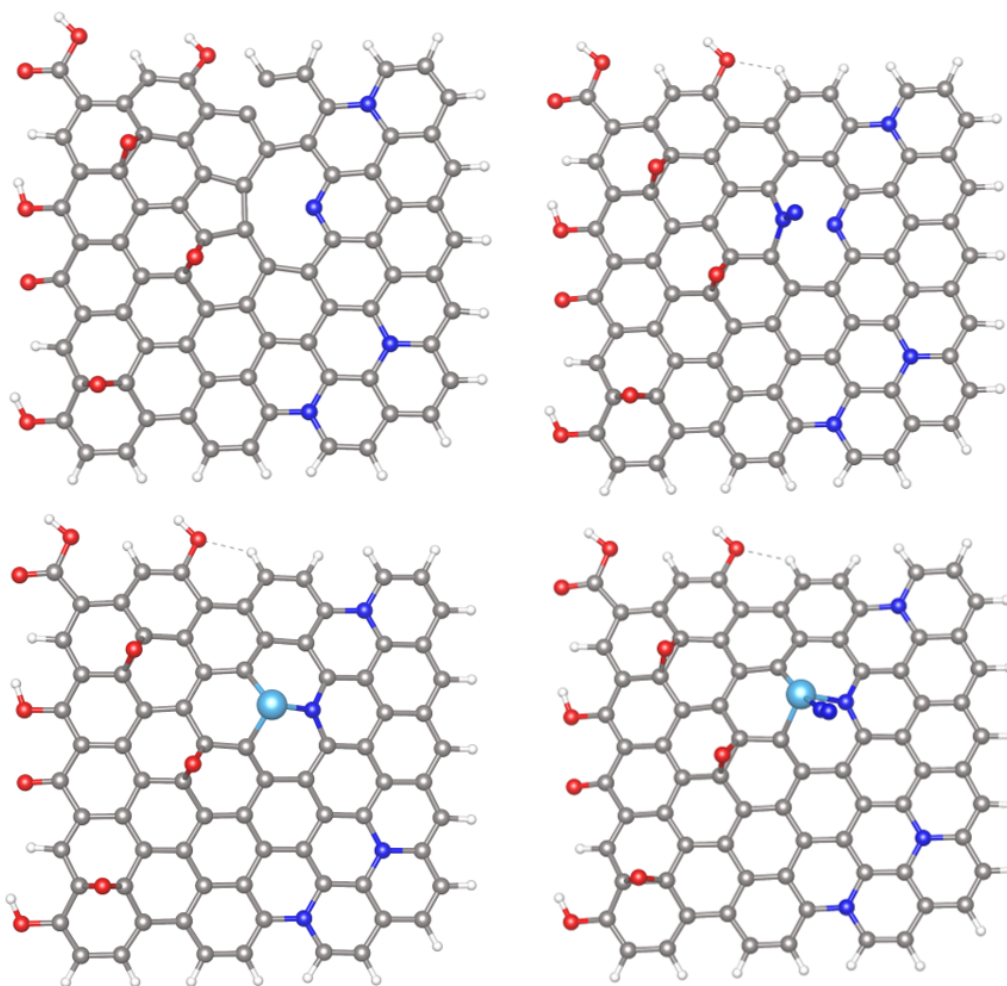


Fig. S7 (a) Optimized geometries of rGO/NC. (b) Optimized geometries of N₂ adsorbed at rGO/NC. (c) Optimized geometries of SA-Ru@rGO/NC. (d) Optimized geometries of N₂ adsorbed at SA-Ru@rGO/NC.

Table S1 Metal content in catalysts.

| Catalyst | Ru content (wt. %) |
|------------------------|--------------------|
| Ru@rGO/NC ₁ | 0.75 |
| SA-Ru@rGO/NC | 0.95 |
| Ru@rGO/NC ₂ | 1 |

Table S2 Comparison of the NRR activity for SA-Ru@rGO/NC with that of other catalysts.

| Catalyst | Electrolyte | FE(%) | Highest NH3 yield rate | Reference |
|------------------------------------|--|-------------|--|-----------|
| FeTPPCI/CS | 0.1 M Na ₂ SO ₄ - PBS | 16.76 ± 0.9 | 18.28 ± 1.6 μg·h ⁻¹ ·mg _{cat} ⁻¹ | 7 |
| 1T-MoS ₂ -Ni | LiClO ₄ | 27.66 | 1.05 mg·min ⁻¹ · cm ⁻² | 8 |
| Bi@C | 0.1 M Na ₂ SO ₄ | 15.10± 0.43 | 4.22± 0.33 μg·h ⁻¹ · mg _{cat} ⁻¹ | 9 |
| Ce _{1/3} NbO ₃ | 0.1 M Na ₂ SO ₄ | 6.87 | 10.34 μg·h ⁻¹ ·cm ⁻² 2 | 10 |
| Vr-ReSe ₂ @CBC | 0.1 M Na ₂ SO ₄ | 42.5 | 28.3 μg·h ⁻¹ ·cm ⁻² | 11 |
| Fe-Ni ₂ P | 0.1M HCl | 7.92 | 88.51 μg·h ⁻¹ · mg _{cat} ⁻¹ | 12 |
| CoMoO ₄ | 0.1 M Na ₂ SO ₄ | 22.76 | 79.87μg·h ⁻¹ · mg _{cat} ⁻¹ | 13 |

References

1. W. Stöber, A. Fink, E. J. Bohn and i. science, *J. Colloid*, 1968, **26**, 62-69.
2. W. S. Hummers Jr and R. E. J. Offeman, *J. Am. Chem. Soc.*, 1958, **80**, 1339-1339.
3. G. Kresse and J. Furthmüller, *Comput. Mater. Sci.*, 1996, **6**, 15-50.
4. P. E. Blöchl, *Phys. Rev. B*, 1994, **50**, 17953.
5. J. P. Perdew, J. A. Chevary, S. H. Vosko, K. A. Jackson, M. R. Pederson, D. J. Singh and C. Fiolhais, *Phys. Rev. B*, 1992, **46**, 6671.
6. S. Grimme, J. Antony, S. Ehrlich and H. J. T. J. o. c. p. Krieg, 2010, **132**, 154104.
7. X. Yang, S. Sun, L. Meng, K. Li, S. Mukherjee, X. Chen, J. Lv, S. Liang, H.-Y. Zang and L.-K. J. Yan, *Appl. Catal., B*, 2021, **285**, 119794.
8. S. B. Patil, H.-L. Chou, Y.-M. Chen, S.-H. Hsieh, C.-H. Chen, C.-C. Chang, S.-R. Li, Y.-C. Lee, Y.-S. Lin and H. J. Li, *J. Mater. Chem. A*, 2021, **9**, 1230-1239.
9. Y. Wan, H. Zhou, M. Zheng, Z. H. Huang, F. Kang, J. Li and R. J. Lv, *Adv. Funct. Mater.*, 2021, **31**, 2100300.
10. X. Hu, Y. Sun, S. Guo, J. Sun, Y. Fu, S. Chen, S. Zhang and J. J. Zhu, *Appl. Catal., B*, 2021, **280**, 119419.
11. F. Lai, W. Zong, G. He, Y. Xu, H. Huang, B. Weng, D. Rao, J. A. Martens, J. Hofkens and I. P. J. Parkin, *Angew. Chem. Int. Ed.*, 2020, **59**, 13320-13327.
12. C. Guo, X. Liu, L. Gao, X. Kuang, X. Ren, X. Ma, M. Zhao, H. Yang, X. Sun and Q. J. Wei, *Appl. Catal., B*, 2020, **263**, 118296.
13. Y. Zhang, J. Hu, C. Zhang, Q. Qi, S. Luo, K. Chen, L. Liu and M. K. J. Leung, *J. Mater. Chem. A*, 2021, **9**, 5060-5066.